Investigation of Ce^{3+} Adsorption by $Sn(OH)_X$ by the Gravimetric Method

Jiejie Yan, Ruixin Chen, Jianshe Wang*

School of Chemical Engineering, Zhengzhou University, Zhengzhou 450000, China

Abstract

In this work, the adsorption of Ce^{3+} by $Sn(OH)_2$, SnO, and $Sn(OH)_4$ was investigated. By comparing the mass of cerium oxalate caused by the adsorbed Ce^{3+}, $Sn(OH)_2$ and $Sn(OH)_4$ have the ability to adsorb Ce^{3+}, while $Sn(OH)_4$ has a stronger adsorption capacity of Ce^{3+}. However, SnO does not have the ability. The possible mechanism of $Sn(OH)_X$ adsorption Ce^{3+} was further discussed. And the result indicates that the hydroxide can adsorb cations by means of anionic groups on its surface in the solution so that the cations can be enriched on the hydroxide surface. The paper provides a new method for adjusting the microstructure of catalysts, which has a promising prospect in the field of catalysts preparation.

Keywords： Adsorption; $Sn(OH)_2$; SnO; $Sn(OH)_4$

1. Introduction

As is well-known, controlling the microstructure of catalysts is critical to the application of catalysts. Various strategies have been employed to controlling the microstructure of catalysts, such as atomic layer deposition (ALD) (Cheng et al., 2015; Song et al., 2019), electro-deposition (Liu et al. 2019; Zheng et al. 2019), and co-precipitation (Qiao et al., 2014). ALD method features atomic-level flexibility in surface structure control but depends heavily on sophisticated equipment and processes. Electro-deposition of metals or metal oxides is cheap and simple in manipulation. However, when preparing electro-catalysts by electrodepositing metal components on metal oxides with poor electrical conductivity, the metal utilization would be lower, limiting the usage of large amounts of metal oxides in electro-catalysis. In contrast, co-precipitation is a simple wet chemical method for preparing most catalysts. Many catalysts are prepared through redox reactions. However, this method is only suitable for substances that can undergo redox reactions. Through the difference in adsorption capacity between two different species, the range of substances used for preparing the catalyst can be expanded. It could be possible to achieve the purpose of regulating the precipitation position and even constructing the interface of different species by in situ adsorption.

SnO_2(Liu et al.,2019; Yang et al.,2019) is one of the most widely used non-carbonaceous metal oxide with appropriate electrical conductivity. Similar to SnO_2, CeO_2 (Bambagionl et al. 2012; Chen et al. 2019; Feng et al. 2019; He et al. 2016; Miller et al. 2016; Tan et al. 2016; Yarmiayev et al. 2019; Yu et al. 2019) is also widely used as excellent co-catalytic component. $Sn(OH)_X$ and Ce^{3+} are important precursors for forming SnO_2 and CeO_2. Therefore, $Sn(OH)_X$ and Ce^{3+} can be used as representatives to study the adsorption between hydroxide and cation.

In this study, Ce^{3+} was enriched with anionic groups on the surface of $Sn(OH)_X$. By measuring the mass of cerium oxalate difference between the blank experiment (no adsorption) and the adsorption experiment, the adsorption capacity of $Sn(OH)_X$ to Ce^{3+} can be estimated.

2. Materials and Methods

2.1 Materials

$SnCl_2{\cdot}2H_2O$, $Ce(NO)_3{\cdot}6H_2O$ and NaOH were obtained from Tianjin Kemiou Chemical Reagent Co., Ltd; HCl was obtained from Zhengzhou Piney Chemical Reagent Factory. All reagents were analytical purity without special notes.

2.2 Preparation of $Sn(OH)_X$

Preparation of $Sn(OH)_2$: 0.8840 g $SnCl_2{\cdot}2H_2O$ was dissolved in dilute HCl solution with pH of approximately 1, into which NaOH solution was added drop-wise under magnetic stirring until pH reaches 7. After filtration, the $Sn(OH)_2$ filter cake was formed.

Preparation of SnO: 0.8840 g $SnCl_2{\cdot}2H_2O$ was dissolved in dilute HCl solution, and NaOH solution was added dropwise to pH reaches 7 with stirring. The turbid liquid was heated until the white precipitate was all converted into black SnO. After natural cooling and filtration, the SnO filter cake was formed.

Preparation of $Sn(OH)_4$: 0. 7237 g $SnCl_2{\cdot}2H_2O$ was dissolved in dilute HCl solution, and NaOH solution was added dropwise to pH reaches 7 with stirring. About 3 mL 30 wt. % H_2O_2 solution was added under stirring to transform $Sn(OH)_2$ to $Sn(OH)_4$. After filtration, the $Sn(OH)_4$ filter cake was formed.

2.3 Experiment of Ce^{3+} adsorption by $Sn(OH)_X$

As shown in Fig. 1, the prepared $Sn(OH)_X$ filter cake was dispersed into 30 mL 9.186 mM $Ce(NO)_3{\cdot}6H_2O$ solution. After stirring and adsorbing for 1 h, 8 mL filtrate were respectively pipetted into two 10 mL centrifuge tubes (mass: m_1 and m_2). Into these two tubes, an appropriate amount of $Na_2C_2O_4$ solution was dropwise added for forming cerium oxalate for analyzing Ce^{3+} content. After centrifugation and removing supernatant, the two tubes with precipitate were vacuum dried at 90 °C until the total mass remains unchanged. The corresponding masses were weighed to be m_1' and m_2', respectively. For comparison, blank experiment was conducted similarly that 8 mL 9.186 mM $Ce(NO)_3{\cdot}6H_2O$ solutions were respectively pipetted into two 10 mL centrifuge tubes (mass: m_3 and m_4). The final total masses of the two centrifuge tubes with dried cerium oxalate were weighed to be m_3' and m_4', respectively.

Fig.1: Schematic diagram of Ce^{3+} adsorption by $Sn(OH)_X$

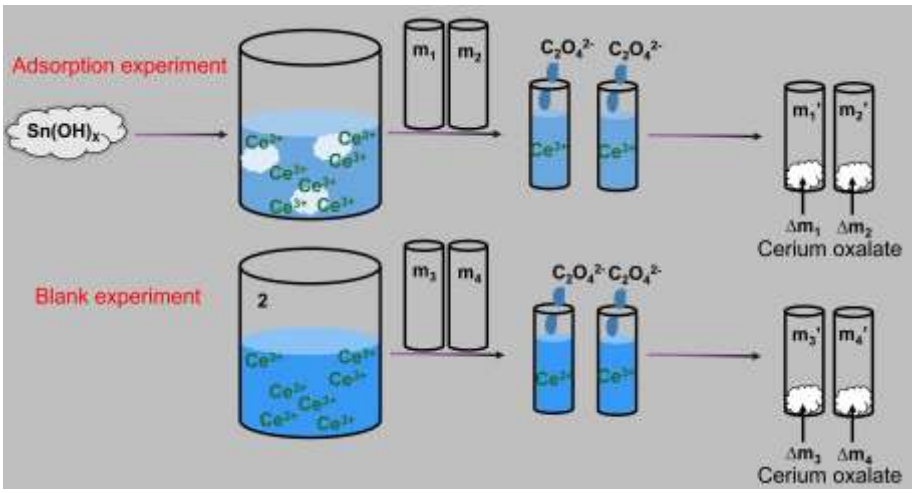

3. Results and discussion

Table 1: The mass analysis of Ce^{3+} adsorption by $Sn(OH)_2$

Adsorption experiment		Blank experiment	
m_1(g)	3.9872	m_3(g)	4.0334
m_1'(g)	4.0126	m_3'(g)	4.0603
$\Delta m_1(m_1'-m_1)$ (g)	0.0254	$\Delta m_3(m_3'-m_3)$ (g)	0.0269
m_2(g)	4.0074	m_4(g)	4.0098
m_2'(g)	4.0331	m_4'(g)	4.0365
$\Delta m_2(m_2'-m_2)$ (g)	0.0257	$\Delta m_4(m_4'-m_4)$ (g)	0.0267
$\overline{\Delta m_1+\Delta m_2}$ (g)	0.0256	$\overline{\Delta m_3+\Delta m_4}$ (g)	0.0268
$\overline{\Delta m_3+\Delta m_4}-\overline{\Delta m_1+\Delta m_2}$ (g)	0.0012		

Table 1 is the mass analysis of Ce^{3+} adsorption by $Sn(OH)_2$. Where Δm_1~Δm_4 is the mass of cerium oxalate. $\overline{\Delta m_1+\Delta m_2}$ is the average mass of cerium oxalate produced by 8 mL remaining Ce^{3+} solution after the adsorption experiment. $\overline{\Delta m_3+\Delta m_4}$ is the average mass of cerium oxalate produced by 8 mL 9.186 mM Ce^{3+} solution. Therefore, $\overline{\Delta m_3+\Delta m_4}-\overline{\Delta m_1+\Delta m_2}$ (0.0012 g) is the mass of cerium oxalate produced by 0.1596 g $Sn(OH)_2$ adsorbed Ce^{3+}, indicating that $Sn(OH)_2$ has the adsorption capacity for Ce^{3+}.

Table 2 The mass analysis of Ce^{3+} adsorption by SnO

Adsorption experiment		Blank experiment	
m_1(g)	3.4378	m_3(g)	3.3698
m_1'(g)	3.4670	m_3'(g)	3.3904
$\Delta m_1(m_1'-m_1)$ (g)	0.0292	$\Delta m_3(m_3'-m_3)$ (g)	0.0269
m_2(g)	3.4537	m_4(g)	3.4213
m_2'(g)	3.4827	m_4'(g)	3.4498
$\Delta m_2(m_2'-m_2)$ (g)	0.0290	$\Delta m_4(m_4'-m_4)$ (g)	0.0285
$\overline{\Delta m_1+\Delta m_2}$ (g)	0.0291	$\overline{\Delta m_3+\Delta m_4}$ (g)	0.0277
$\overline{\Delta m_3+\Delta m_4}-\overline{\Delta m_1+\Delta m_2}$ (g)	-0.0014		

Table 2 is the mass analysis of Ce^{3+} adsorption by SnO. $\overline{\Delta m_3+\Delta m_4}-\overline{\Delta m_1+\Delta m_2}$ (-0.0014 g) is the mass of cerium oxalate produced by 0.1407 g SnO adsorbed Ce^{3+}, indicating that the Ce^{3+} concentration in solution increased after the adsorption experiment. This not only indicates that SnO has no adsorption capacity for Ce^{3+}, but also indicates that a small amount of water evaporation should be accompanied during the adsorption experiment, which causes the Ce^{3+} concentration in solution to increase in the adsorption experiment.

Table 3: The mass analysis of Ce^{3+} adsorption by $Sn(OH)_4$

Adsorption experiment		Blank experiment	
m_1(g)	3.9825 g	m_3(g)	4.0378 g
m_1'(g)	4.0048 g	m_3'(g)	4.0638 g
$\Delta m_1(m_1'-m_1)$ (g)	0.0223 g	$\Delta m_3(m_3'-m_3)$ (g)	0.0260 g
m_2(g)	4.0036 g	m_4(g)	4.0117 g
m_2'(g)	4.0255 g	m_4'(g)	4.0376 g
$\Delta m_2(m_2'-m_2)$ (g)	0.0219 g	$\Delta m_4(m_4'-m_4)$ (g)	0.0259 g
$\overline{\Delta m_1+\Delta m_2}$ (g)	0.0221 g	$\overline{\Delta m_3+\Delta m_4}$ (g)	0.0260 g
$\overline{\Delta m_3+\Delta m_4}-\overline{\Delta m_1+\Delta m_2}$ (g)= 0.0039 g			

Table 3 is the mass analysis of Ce^{3+} adsorption by $Sn(OH)_4$. $\overline{\Delta m_3+\Delta m_4}-\overline{\Delta m_1+\Delta m_2}$ (0.0039 g) is the mass of cerium oxalate produced by 0.1596 g $Sn(OH)_4$ adsorbed Ce^{3+}, indicating that $Sn(OH)_4$ also has adsorption capacity for Ce^{3+}. In addition, $Sn(OH)_4$ has a stronger adsorption capacity for Ce^{3+} than $Sn(OH)_2$ (0.0039 g>0.0012 g).

The possible mechanism of Ce^{3+} adsorption by $Sn(OH)_X$ is shown in Fig. 2. Ce^{3+} adsorption by $Sn(OH)_X$ can be attributed to the fact that there are some anionic groups around $Sn(OH)_X$, such as O^-, OH^-, etc. Ce^{3+} in the solution aggregates to the surface of $Sn(OH)_X$, so that the concentration of Ce^{3+} on the $Sn(OH)_X$ surface liquid film increased, while the concentration of Ce^{3+} in the bulk solution decreased slightly. Since there is no anionic groups on the surface of SnO, Ce^{3+} cannot be adsorbed by SnO.

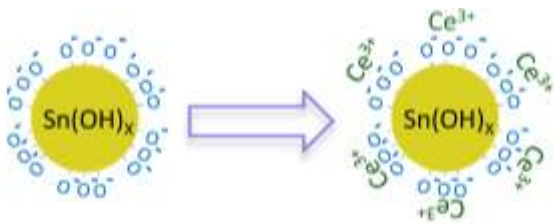

Fig. 2: Schematic diagram of Ce^{3+} adsorption by $Sn(OH)_X$

4. Conclusions

In this research, it was proved by mass analysis that Ce^{3+} can be adsorbed by $Sn(OH)_2$ and $Sn(OH)_4$. Compared with $Sn(OH)_2$, $Sn(OH)_4$ has stronger adsorption capacity because there are more anionic groups on the surface of $Sn(OH)_4$. However, the SnO surface has no anionic groups and cannot adsorb Ce^{3+}. In other words, various hydroxides have not equal adsorption capacities for different cations. This method can be used to microscopically control the structure of catalysts, which brings good news for the preparation of catalysts.

Acknowledgment

This work was supported by Natural Science Foundation of Henan Province (182300410263).

Reference

1. Bambagionl, I. V., Bianchin, C., Chen, Y. X., Filippi, J., Fornasiero, P., Innocenti, M., Lavacchi, A., Marchionni, A., Oberhauser, W., & Vizza, F. (2012). Energy efficiency enhancement of ethanol electrooxidation on Pd–CeO2/C in passive and active polymer electrolyte-membrane fuel cells. Chemsuschem, 5(7), 1266-1273. https://doi.org/10.1002/cssc.201100738

2. Chen, G. J., Dai, Z. F., Sun, L., Zhang, L., Liu, S., Bao, H. W., Bi, J. L., Yang, S. C., & Ma,F. (2019). Synergistic effects of platinum-cerium carbonate hydroxides reduced graphene oxide on enhanced durability for methanol electro-oxidation. J Mater Chem A, 7(11), 2-21. https://doi.org/10.1039/C9TA00226J

3. Cheng, N. C.,Banis, M. N.,Liu, J., Riese, A., Li, X., Li, R. Y., Ye, S. Y., Knights, S., & Sun, X. L. (2015). Extremely stable platinum nanoparticles encapsulated in a zirconia nanocage by area-selective atomic layer deposition for the oxygen reduction reaction. Adv Mater, 27(2), 277-281. https://doi.org/10.1002/adma.201404314

4. Elkholy, A. E., Heakal, F. E., & El-Said, W. A. (2019). Improving the electrocatalytic performance of Pd nanoparticles supported on indium/tin oxide substrates towards glucose oxidation. Appl catal a: Gen, 580, 28-33. https://doi.org/10.1016/j.apcata.2019.04.032

5. Feng, Y. Y., Hu, H. S., Song, G. H., Si, S., Liu, R. J., Peng, D. N., & Kong, D. S. (2019). Promotion effects of CeO2 with different morphologies to Pt catalyst toward methanol electrooxidation reaction. J Alloys Compd, 798, 706-713. https://doi.org/10.1016/j.jallcom.2019.05.287

6. He, Q., Shen, Y., Xiao, K. J., Xi, J. Y., & Qiu, X.P. (2016). Alcohol electro-oxidation on platinum–ceria/graphene nanosheet in alkaline solutions. Int J Hydrogen Energ, 41(45), 20709-20719. http://dx.doi.org/10.1016/j.ijhydene.2016.07.205

7. Liu, W., Lyu, K. J., Xiao, L., Lu, J. T., & Zhuang, L. (2019). Hydrogen oxidation reaction on modified platinum model electrodes in alkaline media. Electrochim Acta, 327,135016. https://doi.org/10.1016/j.electacta.2019.135016

8. Miller, H. A., Lavacchi, A., Vizza, F., Marelli, M., Benedetto, F. D., DÏAcapito, F., Paska, Yet., Page, M., & Dekel, D. R. (2016). A Pd/C-CeO2 anode catalyst for high-performance platinum-free anion exchange membrane fuel

cells. Angew chem int ed, 55(20), 6004-6007. https://doi.org/10.1002/anie.201600647

9. Qiao, B. T., Wang, A. Q., Li, L., Lin, Q. Q., Wei, H. S., Liu, J. Y., & Zhang, T. (2014). Ferric oxide-supported Pt subnano clusters for preferential oxidation of CO in H2-rich gas at room temperature. Acs catal, 4(7), 2113-2117. https://doi.org/10.1021/cs500501u

10. Song, Z. X., Banis, M. N., Zhang, L., Wang, B. Q., Yang, L. J., Banham, D., Zhao, Y., Liang, J. N., Zheng, M., Li, R. Y., Ye, S. Y., & Sun, X. L. (2018). Origin of achieving the enhanced activity and stability of Pt electrocatalysts with strong metal-support interactions via atomic layer deposition. Nano Energy, 53, 716-725. https://doi.org/10.1016/j.nanoen.2018.09.008

11. Tan, Q.,Shu, C. Y.,Abbott, J., Zhao, Q. F., Liu, L,T., Qu, T., Chen, Y.Z., Zhu, H.Y., Liu, Y.N., & Wu, G. (2019). Highly dispersed Pd-CeO2 nanoparticles supported on N-doped core–shell structured mesoporous carbon for methanol oxidation in alkaline media. Acs catal, 9, 6362-6371. https://doi.org/10.1021/acscatal.9b00726

12. Yarmiayev, V., Alesker, M., Muzikansky, A., Zysler,M., & Zitoun, D. (2019). Enhancement of palladium HOR activity in alkaline conditions through ceria surface doping. J electrochem soc, 166(7), F3234-F3239. https://doi.org/10.1149/2.0291907jes

13. Yang, H. L., Li, S. W., Shen, S. H., Jin, Z. M., Jin, J., & Ma, J. T. (2019). Unraveling the cooperative synergy of palladium/tin oxide/aniline-functionalized carbon nanotubes enabled by layer-by-layer synthetic strategy for ethanol electrooxidation. ACS Sustain Chem Eng, 7(11), 10008-10015. https://doi.org/10.1021/acssuschemeng.9b01197

14. Yu, H., Davydova, E. S., Ash, U., Miller, H. A., Bonville, L., Dekel, D. R., & Maric, R. (2019). Palladium-ceria nanocatalyst for hydrogen oxidation in alkaline media: Optimization of the Pd–CeO2 interface. Nano energy, 57, 820-826. https://doi.org/10.1016/j.nanoen.2018.12.098

15. Zheng, J. N., Huang, K. L., Hou, G. Y., Zhang, H. B., & Cao, H. Z. (2019). A highly active Pt nanocatalysts supported on RuO2 modified TiO2-NTs for methanol electrooxidation with excellent CO tolerance. Int J hydrogen energ, 44(59), 31506-31514. https://doi.org/10.1016/j.ijhydene.2019.10.048